DOI 10.5162/iCCC2026/1.4

Berstdruckvorhersage von faserverstärkten Druckbehältern anhand von Schallemissionen

Burst pressure prediction with Acoustic Emissions on composite pressure vessels

Emanuel D. Kästle, Ali Ghaznavi, Eric Duffner
Bundesanstalt für Materialforschung und -prüfung (BAM), 3.5 Sicherheit von Gasspeichern und Gefahrguttanks, Berlin, Deutschland
emanuel-david.kaestle@bam.de

Kurzfassung

Neue Arbeiten zeige eine Methode zur Vorhersage der Versagenslast von kohlenstofffaserverstärkten Polymerwerkstoffen (CFRP) mittels Schallemission auf. Dies ermöglicht eine zerstörungsfreie Bewertung der Restfestigkeit von Druckbehältern und trägt so zur Verbesserung der Betriebssicherheit bei. Der hier betrachtete Datensatz umfasst sieben kleinformatige CFRP-Proben unter Zugbelastung sowie fünf vollständige CFRP-Druckbehälter vom Typ IV. Alle Prüfkörper wurden in periodischen Lade- und Entladezyklen getestet, um charakteristisch Kennwerte bei unterschiedlichen Laststufen zu erfassen. Auf Basis dieser Daten wird ein neuronales Netz trainiert, das die Kennwerte mit den Laststufen relativ zur Versagenslast verknüpft. Die Ergebnisse zeigen, dass Vorhersagen auch über unterschiedliche Prüfkörper hinweg möglich sind; Modelle, die mit Probendaten trainiert wurden, können den Berstdruck vollständiger Behälter vorhersagen – und umgekehrt. Einschränkungen im Hinblick auf potenzielle Verzerrungen und die Notwendigkeit aussagekräftiger Unsicherheitsabschätzungen werden diskutiert und bleiben eine Herausforderung für zukünftige Arbeiten.

Abstract

Recently, a method for predicting the failure load of carbon fiber reinforced polymer (CFRP) materials has been presented. The method relies on passive acoustic emission (AE) monitoring during loading. This approach could be used in the non-destructive evaluation of the residual strength of pressure vessels and therefore improve the operational safety. A test dataset is obtained from 7 small-scale CFRP specimens, subjected to tensile load, as well as 5 full CFRP type IV pressure vessels. All test objects are equipped with AE sensors and periodically loaded and unloaded to get characteristic AE-related ratios at different load steps. Using these data, we train a neural network to link AE-derived ratios to load levels relative to the failure load. It is shown that predictions are possible, also across different test objects, i.e. trained with specimen data, burst pressure predictions for full vessels are feasible and vice versa. We discuss limitations related to potential biases and the need for meaningful uncertainty estimation, which remain open for future work.

1 Introduction

The global energy system is transitioning toward sustainability. In this context, hydrogen has gained prominence as a versatile energy carrier, offering a pathway to decarbonize sectors that are difficult to electrify, such as heavy industry, long-haul transportation, and seasonal energy storage [1]. Compressed hydrogen (up to 700 bar) is widely used for onboard storage in fuel cell vehicles and transport trailers. To achieve safe and efficient storage under these conditions, type IV carbon fiber reinforced polymer (CFRP) pressure vessels have become the industry standard [2]. These composite vessels offer an exceptional strength-to-weight ratios, corrosion resistance, and durability under cyclic loading. Since pressure vessels represent a safety critical element of the hydrogen value chain, they must undergo regular inspections or must be operated with a pre-defined limited-service lifetime. Inspections are costly and often require destructive testing of sample vessels. Vessels that have reached the end of their service lifespan, may still fulfill necessary safety criteria so that disposal implies a waste of valuable resources. A major factor for the costs and CO2 emissions of CFRP vessels is the energy-intense carbon fiber production [2]. At the same time, recycling options are still very scarce or inefficient. The BAM is therefore interested in developing a method for non-destructive testing of CFRP vessels to improve the operational safety and to avoid long out-of-service periods during inspection. Recently, Sause et al. [3, 4] have presented a method for the failure load prediction of CFRP specimen and shown that it is also applicable on full vessel scale. This method is based on testing with acoustic emissions (AE), a non-destructive testing method based on the occurrence of ultrasonic signals when a material is subjected to a force. At BAM, we have conducted preliminary tests on several CFRP specimens under tensile load and on two different sizes of type IV CFRP vessels from different manufacturers. The results of these test will be presented, and the accuracy of the failure load prediction will be discussed. The terms failure load (for specimens) and burst pressure (for vessels) are used interchangeably throughout this work.

DOI 10.5162/iCCC2026/1.4

2 Method

The applied method for the load failure prediction is based on the works of Sause et al. [3, 4]. The following summarizes the method with minor deviations. AE data are recorded during alternating loading/unloading to compute Felicity [5], Shelby, and energy-related ratios (Fig. 1).

Following Sause et al. [3], the Felicity ratio is calculated from a percentage threshold of the total number of hits recorded during one load/pressure step. A hit describes one short ultrasonic burst signal, emitted by the material and recorded at the AE sensors. The Felicity ratio is therefore given by:

$$FR_{n\%} = L_{n\%}/L_0$$

The variable n gives the threshold value so that $L_{5\%}$ is the load level where the threshold of 5% of the signals is exceeded. Different ratios at thresholds of 5, 10, 15 and 20% are extracted from the data [3]. A fifth ratio is given by the mean of the four aforementioned ones, FR_{mean}. The Shelby ratio (SR) is based on a similar concept as the FR, but counts the number of hits during unloading, with threshold levels at 80, 85, 90 and 95% of the total number of hits. A fifth ratio will be SR_{mean}. The third type of AE-based ratios are the energy (ENE), signal strength (SST) and amplitude (AMP) ratios. The definition of these parameters follows the one implemented in the Vallen software (www.vallen.de). The energy ratio is given as the load level where the cumulated energy of the current load increase, E_1, exceeds 80% of the cumulated energy of the previous load step, E_0, relative to the previous load maximum, L_0:

$$ER = L_{E_1 \geq 0.8E_0}/L_0$$

The 0.8 factor, absent in [3], prevents undefined ratios when current energy does not exceed previous energy. The amplitude and signal strength ratios are calculated analogously. This results in a total of 13 ratios which are used in the burst pressure prediction approach.

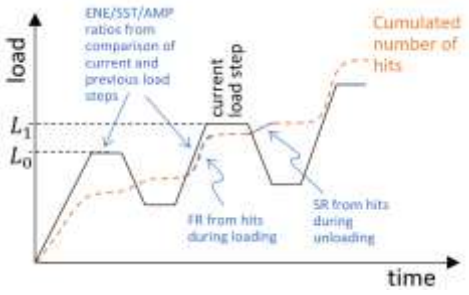

Figure 1 Schematic loading and unloading profile used in this work. FR and SR are based on the cumulated number of hits during loading and unloading. The other ratios are based on cumulated energies, signal strength and amplitudes.

As shown in Fig. 1, there is no complete unloading after each load maximum, which is different from [3]. The load is decreased by a factor of 0.5. This means that the smallest possible ratios are 0.5. The largest possible value for the Shelby ratios is always 1, which follows from the definition above. For the Felicity and ENE/SST/AMP ratios, it is given by L_{i+1}/L_i. In our tests, $L_{i+1} - L_i$ is kept constant over the load profile, so that the largest possible value for the ratio decreases with increasing load.

Ratios are input to a two-layer neural network [3]. The network has 13 inputs (or 8 without Shelby ratios), one hidden layer (10 nodes), and an output layer with two nodes, representing the mean and the standard deviation of the load ratio (LR) which is defined as:

$$LR = L_i/L_{failure}$$

where L_i is the current load level (Fig. 1). Using the LR instead of absolute values makes the model more generalizable. The LR values required for model training are given from the true failure loads (burst pressures) of the tested specimens (vessels). A single prediction could estimate failure load, but this introduces high uncertainty. Therefore, several predictions should be made, from which the average failure load is calculated by a linear regression (Fig. 2). The slope is computed via weighted linear regression using LR standard deviations as weights. The lower and upper boundaries of the failure load are estimated from the mean slope ±2 standard deviations.

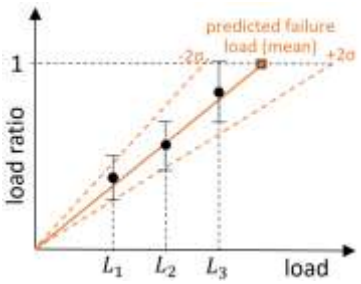

Figure 2 Schematic failure load prediction from three predicted LRs . The dashed orange lines indicate slope lines ±2 times standard deviations (σ).

3 Data

The dataset includes seven CFRP specimens with alternating 0°/90° fiber layers, tested under tensile load. The free length of samples (between the reinforcement tabs) is 15 cm, the width is 2.5 cm and the thickness approx. 2 mm (Fig. 3). Each sample is monitored with four Vallen VS900-M broadband sensors connected to Vallen AEP5 preamplifiers and a Vallen AMSY-6 data logger to record the AE signals during testing. Additionally, five vessels are tested, each with 15 identical sensors and the same measurement setup and AE equipment. Three sensors are glued onto each dome and nine sensors are glued with approximately equal distance onto the cylindrical surface of the vessels using hot melt adhesive. Two small vessels (~50 cm × 15.5 cm, labeled ‘S’) and three large vessels (~90 cm × 23.5 cm, labeled ‘L’) were hydraulically tested.

An example of the extracted ratio data is given in Fig. 4. The Felicity and energetic ratios clearly follow a trend, which is usable for predictions, while the extracted Shelby ratios are more scattered. The variability may be due to the lower number of hits during unloading phases. Therefore, the Shelby ratios will not be used in the following. Also, Sause et al. [4] did not use Shelby ratios in their more recent work. On the one hand, the FR and ER trends depend

DOI 10.5162/iCCC2026/1.4

on the load levels, since the largest possible values are L_{i+1}/L_i. On the other hand, the trends are controlled by a change in AE activity at different load levels. The dataset comprises ratio data at load ratios close to 1, i.e. the failure load. This is, because tests on specimens and on vessels S1 and S2 were conducted until failure with acoustic emission sensors attached. For the L1 to L3 vessels, the tests were stopped at a pressure close to bursting and the sensor were removed. The burst test was conducted only afterwards. The obtained failure loads for the CFRP specimens are shown in Fig. 4.

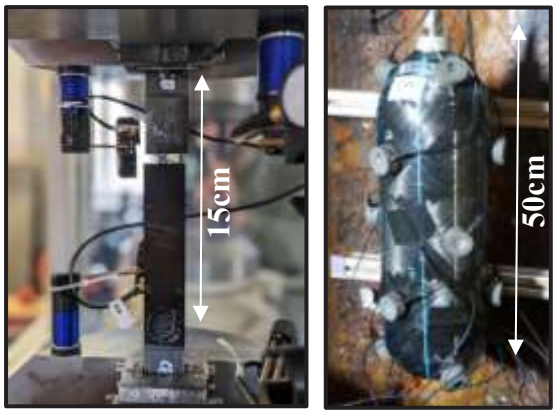

Figure 3 Test setup for tensile specimen testing (left) and for a full vessel of type S (right). 15 sensors are glued to the surface of the vessel.

The shown ratio values are calculated from all available sensors taken together. This gives more stable values and reduces the effect from outliers. However, it is also possible to treat the data for each sensor separately which can add to the estimations of the prediction uncertainty or can be used to identify regions with higher AE activity [4]. Despite the factor of 0.8 for the ENE/SST/AMP ratios, on some occasions, no valid values can be extracted where E_l<E_0 (*ER* equation above). A valid datapoint includes all 5 FRs and 3 energetic ratios. The total number of valid datapoints is 88.

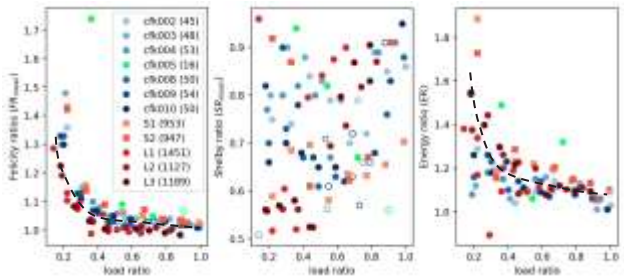

Figure 4 FR_{mean}, SR_{mean} and ER data extracted from the load/pressurization tests. The other extracted ratios are not shown for the sake of clarity. Open circles/squares indicate incomplete datapoints, because of missing ER values. Labels *cfk* correspond to tensile specimen data, *L* and *S* describe large and small vessel data. The average data trends are highlighted with dashed lines. The failure loads (in kN) and the burst pressures (in bar) are given in brackets in the legend behind each sample. The sample data highlighted in green is discussed in section 5.

4 Results

Several results are presented, for different combinations of training and testing datasets. Since the number of datapoints is relatively small, the test dataset also serves as validation dataset. Training is stopped when the validation residual starts being consistently above the training residual. With larger datasets, a separation of validation and test datasets, and a validation dataset taken from the training data, should be preferred.

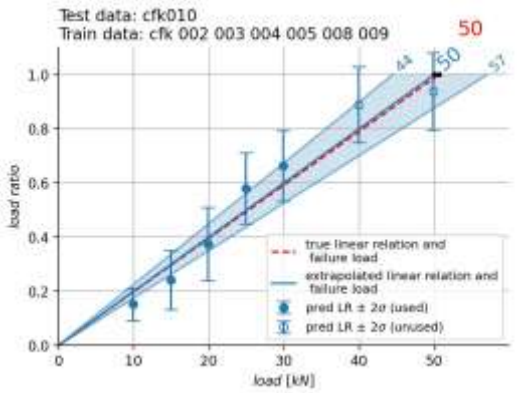

Figure 5 Failure load prediction for sample cfk010 with a model trained on the remaining 6 cfk samples.

Figure 5 gives an example only using CFRP specimen data. For this example, the prediction (49 kN) is very close to the true failure load at 50 kN. In the diagram, all load ratio predicted by the neural network are plotted together with their estimated standard deviation. In the following linear regression step, the last two datapoints are not used, since in an actual application, the test would be stopped, and a prediction would be made before critical loads are reached. In this and all the following examples, we do not consider predicted load ratios above 70% of the true failure load in the linear regression. We choose this threshold to simulate a realistic test which is stopped at a safe margin before failure.

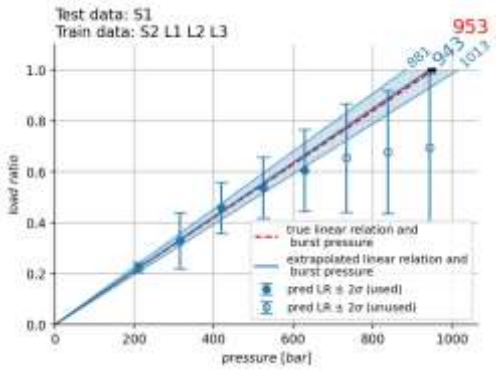

Figure 6 Failure load (burst pressure) prediction for vessel S1 with a model trained on the remaining 4 vessels.

In Figure 6, a similar test is presented using only vessel data. The predicted burst pressure is about 55 bar below the true burst pressure. An offset in the LRs is visible, more pronounced at larger pressures. This could lead to

DOI 10.5162/iCCC2026/1.4

larger errors if more LR values (beyond the 70% limit) were used in the linear regression. This is likely to be explained with the offset in the S- and L-vessel data, where ratios extracted for the S vessels consistently show slightly higher ratios (Fig. 4). A reason for this is discussed below.

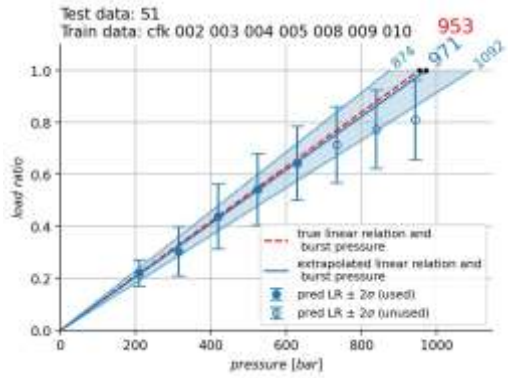

Figure 7 Failure load (burst pressure) prediction for vessel S1 with a model trained on CFRP tensile specimen.

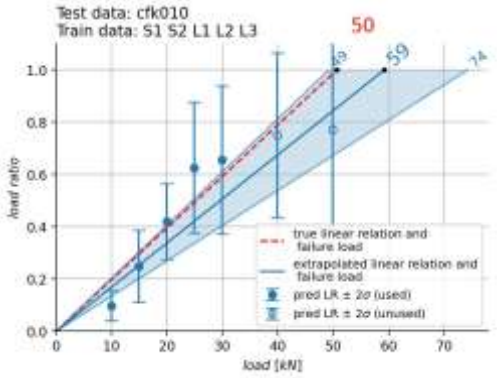

Figure 8 Failure load prediction for sample cfk010 with a model trained on 5 vessel datasets.

Finally, Figs. 7 and 8 present mixed prediction results for training datasets based on specimen data and predictions for vessel data, and vice versa. The predicted failure loads / burst pressures are within the given uncertainty margins in both cases. This shows that predictions are possible across the different test objects, even though the uncertainties may be high.

5 Discussion

The results presented in the preceding section show that the failure load prediction method works and can even be applied across different CFRP sample types. Given the similar behavior of the ratio data presented in Fig. 4, a positive result was to be expected. There are, however, some limitations that deserve attention. Currently, the dataset is relatively small, so that the results would change if only a few additional data points were introduced. This means that the predictions, including the predicted uncertainties are not very reliable, yet. A proper dataset should probably include serval dozens of tested specimens, ideally subjected to other tests (e.g., bending) and with different layups and defects. A much larger number and variety of vessels would further help to estimate the reliability of the method. With the current approach of averaging data from all sensors, local weak zones may go undetected (e.g., from impacts), so that obtaining ratios separately for different sensors, or even localized to certain regions on the vessel surface could be beneficial [4].

The uncertainties, estimated from the slope ±2σ only give a very basic guess for the true uncertainty. The resulting uncertainties only depend on how well the point align on a linear relation, without taking the predicted load ratio standard deviations into account. A more rigorous approach could be provided by a Bayesian linear regression.

The load/pressure release is 50% in every step (Fig. 1), which is different from Sause et al. [3] who unload complete. This results in longer testing times, but also more signals, and larger spread in the Felicity, Shelby and energetic ratios from low to high loads. The fact that the Felicity ratios hardly ever go below 1 in this work is related to the limited unloading in combination with the pristine condition of the specimens/vessels that have never been loaded before: Most signals are emitted when high load levels are reached for the first time. The larger spread from complete unloading could therefore help to improve the prediction accuracy. Small deviations from the planned loading profile can significantly influence the obtained ratios. This includes shorter/longer holding phases between loading and unloading and deviations towards too high or too low loads which did happen in our experiments, e.g. by small leakages or overshooting of the pressurization device. A very severe influence is further observed if loading is repeated, e.g. a vessel which has already seen pressures up to 1000 bar, and then ratio data is extracted for different steps below that level. This results in ratios that deviate strongly from the profile shown in Fig. 4. The current method is therefore only applicable for pristine CFRP materials.

For the CFRP vessel datasets, there appears to be a small offset in the ratio data between S and L vessels (Fig. 4). It is also evident that a similar offset occurs for the one sample with significantly lower failure load (cfk005). This can be easily understood when considering that the x-axis in Fig. 4 gives the load ratio. At a given load step, a reduced failure load results in a higher load ratio so that all datapoints are shifted to the right. As shown in Fig. 6, this can cause a bias in the predicted values. This phenomenon is thus related to the fact that the observed trend in the ratio data is mainly caused by having fixed $L_{i+1} - L_i$ steps and consequently a reduction in the L_{i+1}/L_i ratios with higher load. A correction for this effect or additional inputs to the neural network might therefore be desirable to obtain more reliable results.

6 Conclusions

An implementation of the failure load prediction method first introduced by Sause et al. [3] is presented. By comparing data from CFRP specimens under tensile load, as well as from two types of CFRP pressure vessels, it is

shown that good predictions are possible, even across different test object types and small sample sizes. The presented dataset is relatively small (7 specimens, 5 vessels), nevertheless the true failure loads are always within a ±2σ range from the predicted values. Future developments should take more diverse CFRP tests and specimens into account, improve the estimation the prediction uncertainty, and consider a careful re-evaluation of the input ratios which are, in parts, too scattered (Shelby ratios) or can produce prediction biases (Felicity, energetic ratios).

7 Acknowledgements

We want to thank the project partners and colleagues involved in the DAVID project and at BAM who conducted many of the required tests. This work was supported by the German Federal Ministry of Economic Affairs and Energy within the DAVID project (03LB3099C) and the BTU-BAM Graduate School „Trustworthy Hydrogen“.

8 References

[1] S. O. Akpasi, I. M. S. Anekwe, E. K. Tetteh, U. O. Amune, S. I. Mustapha und S. L. Kiambi, „Hydrogen as a clean energy carrier: advancements, challenges, and its role in a sustainable energy future,“ *Clean Energy,* Bd. 9, pp. 52-88, January 2025.

[2] T. Q. Hua, R. K. Ahluwalia, J.-K. Peng, M. Kromer, S. Lasher, K. McKenney, K. Law und J. Sinha, „Technical assessment of compressed hydrogen storage tank systems for automotive applications,“ *International Journal of Hydrogen Energy,* Bd. 36, pp. 3037-3049, February 2011.

[3] M. Sause, S. Schmitt und S. Kalafat, „Failure load prediction for fiber-reinforced composites based on acoustic emission,“ *Composites Science and Technology,* Bd. 164, p. 24–33, August 2018.

[4] M. G. R. Sause, S. Schmitt, B. Hoeck und A. Monden, „Acoustic emission based prediction of local stress exposure,“ *Composites Science and Technology,* Bd. 173, pp. 90-98, March 2019.

[5] T. J. Fowler, „Acoustic Emission of Fiber Reinforced Plastics,“ *Journal of the Technical Councils of ASCE,* Bd. 105, pp. 281-289, 1979.